LINKOAHO, M. V. (1971). *Philos. Mag.* **23**, 191–198.
STEVENS, E. D. (1974). *Acta Cryst.* A**30**, 184–189.
STEWART, A. T. & BROCKHOUSE, B. N. (1958). *Rev. Mod. Phys.* **30**, 250–255.
WAKOH, S. & KUBO, Y. (1980). *J. Phys. F*, **10**, 2707–2715.
WAKOH, S. & YAMASHITA, J. (1971). *J. Phys. Soc. Jpn*, **30**, 422–427.
WEISS, R. J. & DEMARCO, J. J. (1965). *Phys. Rev. A*, **140**, 1223–1225.
ZACHARIASEN, W. H. (1967). *Acta Cryst.* **23**, 558–564.

Acta Cryst. (1981). A**37**, 701–710

An Oscillation Data Collection System for High-Resolution Protein Crystallography

BY M. F. SCHMID, L. H. WEAVER, M. A. HOLMES, M. G. GRÜTTER, D. H. OHLENDORF, R. A. REYNOLDS, S. J. REMINGTON* AND B. W. MATTHEWS†

Institute of Molecular Biology and Department of Physics, University of Oregon, Eugene, Oregon, USA

(*Received* 13 *November* 1980; *accepted* 25 *March* 1981)

Abstract

An oscillation data collection system for protein crystallography is described. The system consists of a modified Enraf–Nonius precession camera with cylindrical cassette, and stepping motor driven by a flexible microprocessor control system. The X-ray source is graphite-monochromatized radiation from an Elliott GX-21 rotating-anode generator run at 5·5 kW on a focal spot measuring 0·5 × 5·0 mm. The potential advantages of using a relatively large focal spot in conjunction with a graphite monochromator are discussed. Conditions for optimum collimation and X-ray intensity are considered, and it is shown that appropriately designed collimators with adjustable apertures can have substantial advantages over commercially available pinhole collimators. The oscillation films are processed by a procedure based on that of Rossmann [*J. Appl. Cryst.* (1979), **12**, 225–238]. Determination of the initial alignment of the film is facilitated by a pair of reference pins incorporated in the cylindrical cassette. These pins ensure that the position of the film in the cassette is known, and avoid the need for fiducial marks. The crystal alignment and film measurement technique is fully automatic, requiring no prior input other than the approximate starting orientation of the crystal, the approximate unit-cell dimensions, and the angular oscillation range. An alternative method for the determination of crystal orientation is proposed which has been found to be somewhat superior to that of Rossmann, especially for smaller unit cells.

1. Introduction

The use of screenless X-ray photography for the rapid, efficient measurement of diffraction data from protein crystals is well established, and an increasing number of laboratories have developed, and are using, such techniques (*e.g.* Xuong & Freer, 1971; Arndt, Champness, Phizackerley & Wonacott, 1973; Schwager, Bartels & Jones, 1975; Rossmann, 1979; Wilson & Yeates, 1979; and the collection of papers in Arndt & Wonacott, 1977).

In this paper we wish to describe an oscillation data collection system we have developed which includes a number of features we have found to be of value, and may be of interest to other laboratories.

These features include graphite monochromatization to reduce background and enhance crystal life, the use of a broad-focal-spot X-ray generator to reduce exposure times by a factor of four, improved collimation geometry, and cylindrical cassettes for high-resolution data collection. The film scanning program, adapted from that of Rossmann (1979), permits the accurate determination of crystal alignment from the oscillation photograph itself, with no prior input other than the approximate orientation of the crystal. We have adopted an alternative strategy for refinement of the crystal orientation which we have found to work better than the 'convolution' procedure developed by Rossmann for virus crystal photography.

The basic hardware consists of two Enraf–Nonius precession cameras, modified for oscillation photography, each controlled by a microprocessor. The cameras are mounted on an Elliott GX-21 rotating-anode generator with Charles Supper graphite monochromators. Films are scanned by an Optronics P3000 rotating-drum scanner interfaced to a Varian V76

* Present address: Max-Planck-Institut für Biochemie, D-8033 Martinsried bei München, Federal Republic of Germany.
† To whom correspondence should be addressed.

0567-7394/81/050701-10$01.00

computer. The V76 computer is used simply to write optical densities on magnetic tape. Typically, nine 7 × 5 in (171·5 × 122·5 mm) films, scanned with a 100 μm raster, can be accommodated on one 2400 ft, 800 bpi tape. Data processing and data reduction are performed on a VAX 11/780 computer.

2. The oscillation camera

The oscillation–rotation cameras consist of modified Enraf–Nonius precession cameras with a stepping motor driven by a microprocessor controller, patterned after those used in Dr Robert Huber's laboratory (Huber, personal communication; Arndt & Wonacott, 1977, p. 30).

The possibility of precession and oscillation geometry on the same camera permits the use of precession as well as still photographs during the initial alignment of the crystal. Also, with some space groups we have found it useful to take a precession photograph of one zone (*e.g.* the centrosymmetric zone) of the same crystal which has been used for oscillation photography. On the other hand, the use of a modified precession camera does not have the convenience of a carousel with a number of pre-loaded cassettes as used in the commercially available oscillation camera systems. Cylindrical cassettes with a radius of 80 mm permit data collection to Bragg spacings of 1·6 Å on 175 × 125 mm sheets of film. A cylindrical cassette has obvious advantages over a flat cassette for high-resolution data collection, and has simpler geometry than that of *V*-shaped cassettes (Arndt & Wonacott, 1977, p. 27). The spot shape is more constant and the obliquity corrections are simpler for a cylindrical cassette than for a *V*-shaped one.

In commercially available cassettes, fiducial marks are made on the film either by allowing light to enter narrow holes, which often produces an ill-defined reference mark, or by using an ancillary X-ray source to direct X-rays through the fiducial holes onto the film. The latter method is not only inconvenient, but does not always work successfully. It is a common and very frustrating experience to find that the fiducial marks on the film are sufficiently out of register with the actual diffraction pattern that one cannot locate reflections at their expected positions on the film (*e.g.* Arndt & Wonacott, 1967, pp. 25–26; Wilson & Yeates, 1979; Rossmann, 1979). A method of avoiding these difficulties, which we have found to work well, is to incorporate a pair of metal pins in the film cassette itself in exactly the same relative positions that they occupy on the film scanner. The scanner mounting holes are punched in the films *before* they are loaded in the cassette. Then, when the film is subsequently mounted on the film scanner, it is automatically aligned in precisely the same way that it was in the cassette during X-ray photography. Since the film scanner starts at an arbitrary position when it scans across the film, it is necessary to have a reference mark on the film to define the origin in the horizontal direction. The spot made by the direct beam is very convenient for this purpose. In principle, one can dispense with the direct-beam mark if the background on the film is dark enough for the film scanner to detect the shadow on the left and right sides of the film made by the edge of the cassette. Either of these steps in optical density can also serve to define the horizontal origin.

There is another advantage in knowing the precise orientation of the film in the cassette. To a close approximation, a rotation of the film in the cassette is equivalent to a rotation of the crystal about the X-ray beam. Therefore a rotation of the film could be incorrectly attributed to an apparent rotation of the crystal, which in turn will lead to errors in the Lorentz–polarization correction and in other geometrical factors.

The stepping motor for the oscillation or rotation motion is driven by a microprocessor controller which we have found to be both flexible and very reliable. Advantages of current microprocessor technology have been described by Reeke (1977). The controller has a repertoire of commands whereby the user can drive the crystal to a specified angle, and specify the oscillation range, speed of rotation, number of cycles, and so on. Should the X-ray generator turn off during an exposure, the microprocessor enters a 'wait' mode, giving the user the option of resuming the exposure when the generator is returned to power.

3. Collimation

Conditions for optimum collimation have been discussed at length by Huxley (1953) and by Arndt & Sweet (1977). In their discussion it is assumed that the protein crystal is smaller than the exit pinhole of the collimator, but in practice many laboratories have found it advantageous to use crystals much larger than the collimator diameter, both to maximize the intensity of reflections on the film and also to permit multiple exposures of different parts of a single crystal. As shown below, some commercially available collimators are not well suited to this geometry, and there are advantages in using appropriately designed adjustable collimators.

A schematic diagram of the collimation system with a graphite monochromator is shown in Fig. 1. The horizontal and vertical dimensions of the X-ray focal spot are denoted f_x and f_y. With a monochromator present, it is, in general, necessary to place an aperture as close to the exit of the monochromator as possible in order to reduce the divergence of the monochromated beam (see the following section). In practice, this

aperture can be a simple pinhole made by piercing a lead sheet with a needle, and mounted on an X–Y translation stage to facilitate alignment. For generality, we denote the horizontal and vertical dimensions of the aperture as f'_x and f'_y. The source aperture of the collimator is usually large (about 1 mm) and plays no part in the collimation.

As discussed by Arndt & Sweet (1977), when the protein crystal is smaller than the specimen aperture ($a_x < a'_x$), simple geometry shows that the width of the spot on the film is

$$w_x = a_x + (a_x + f'_x)\frac{d}{s}. \quad (1)$$

If, however, the crystal is larger than the specimen aperture ($a_x > a'_x$), then the spot width will be

$$w_x = a'_x + (a'_x + f'_x)\frac{d'}{s'}. \quad (2)$$

For Enraf–Nonius collimators, for example, the specimen aperture is about 30 mm from the crystal, which results in a considerable increase in spot size. Substituting some typical numbers (s = 120 mm, d = 80 mm, f'_x = 0·45 mm) a large crystal with collimator aperture a'_x = 0·4 mm will produce a spot of width 1·44 mm, whereas a crystal measuring 0·4 mm a side will produce a spot on the film measuring 0·97 mm. The larger spot size is undesirable, not only because the diffracted X-rays are spread over a larger area, but also because spot overlap limits resolution.

The obvious solution is to have the specimen aperture as close to the crystal as possible. In addition, it is desirable to be able to adjust the vertical and horizontal dimensions of the specimen aperture independently. If, for example, one had a crystal with a long reciprocal axis in one direction, but not the other, then one might wish to use a narrow aperture in this direction in order to resolve the spots, but retain a wider aperture in the other direction in order to increase the total scattered intensity, and the resultant accuracy of intensity measurement.

Both these objectives can be met by using collimators similar to those proposed by Love, Hendrickson, Herriott, Lattmann & McCorkle (1965). As shown in Fig. 2, the adjustable apertures are obtained with polished flat-faced set screws. The length of the collimator is such that it ends as close to the crystal as possible (about 1 mm). Also the adjustable apertures are set as far forward in the collimator as possible. We have found that the guard apertures are not strictly necessary, presumably because the defining apertures are quite flat, and act as their own guards. This means that one only needs to use one vertical aperture and one horizontal aperture. Obviously, the two sets of adjustable screws closest to the protein crystal are the ones used, bringing the defining aperture even closer to the crystal. In practice, the adjustable collimators are easier to make than the standard ones, since the difficult step of drilling the pinhole is avoided. The alignment of the adjustable apertures is best accomplished by mounting the collimator with a light behind, and viewing it from the front with a low-power microscope. The collimator mount and microscope of a Weissenberg camera are ideal for the purpose. Centering of the aperture is checked by rotation. Since the collimators are easy to make it is convenient to have a selection available with commonly used aperture sizes.

It remains to select the actual aperture size, effective focal-spot size, and the distance s' in Fig. 1. Much of the treatment of pinhole collimation given by Arndt & Sweet (1977) is germane, and can be consulted. In practice, the optimum collimator aperture size is 0·3–0·5 mm, smaller values being used only when mitigated by cell edges longer than 150 Å or so. It has to be remembered that if the monochromator crystal is vertical, then the vertical divergence of the X-ray beam is from the focal spot and not from the monochromator. (There is a small additional divergence α,

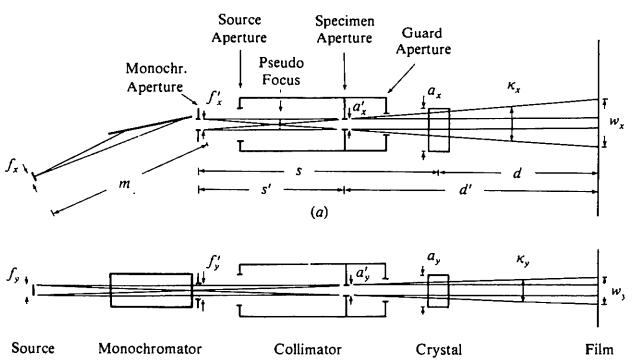

Fig. 1. Schematic illustration of collimation geometry when a monochromator is present and when the dimensions of the crystal exceed those of the specimen aperture of the collimator. The monochromator is mounted in the vertical plane. (*a*) Plan. (*b*) Elevation.

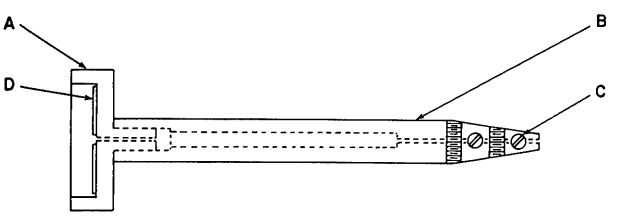

Fig. 2. Adjustable X-ray collimator patterned after that described by Love *et al.* (1965). The components are as follows. *A* Brass cup. *B* Brass tube with optional taper. The taper is usually not necessary for oscillation photography. *C* Flat-faced, polished, (4-80) brass screws, to provide adjustable collimation. Usually the front pairs of screws can be used as both defining and guard apertures (see text). *D* lead shield. A full set of drawings for the collimator is available on request from the authors.

discussed in the following section, owing to the mosaicity of the graphite crystal.) Therefore, the vertical crossfire (Fig. 1*b*) is

$$\kappa_y = \frac{(f_y + a'_y)}{s' + m} + \alpha, \tag{3}$$

whereas the horizontal crossfire (Fig. 1*a*) is

$$\kappa_x = \frac{f'_x + a'_x}{s'}. \tag{4}$$

For a 0·5 mm focal spot, 0·4 mm collimator aperture, $(s' + m)$ equal to its minimum practical value of about 220 mm, and $\alpha = 0{\cdot}06°$ (see next section), the vertical crossfire has the reasonably low value of 0·29°, as is desirable to minimize the spindle rotation required to sweep through each Bragg reflection of the protein crystal. Decreasing the focal-spot size (*e.g.* to 0·2 mm) will decrease the vertical crossfire but not the horizontal. As discussed in the next section, use of a small focal spot may unnecessarily reduce useful beam intensity.

Up to a point, the diameter of the pinhole (f'_x and f'_y) can be increased in order to maximize beam intensity, commensurate with resolving reflections on the film. Increasing f'_x will increase intensity, but will also increase the horizontal dimension of the spots on the film (equation 2). In the vertical direction, f'_y does not define the useful X-ray beam (Fig. 1*b*). Ideally, f'_y should be just large enough not to restrict the limiting cone of X-rays between the focal spot and the specimen aperture (Fig. 1*b*). Decreasing f'_y below this value will reduce beam intensity but will not reduce the crossfire, which is determined by f_y and a'_y (equation 3). In principle, f'_y could be eliminated (*i.e.* f'_x could be a vertical slit) but the aperture f'_y does prevent unnecessary radiation exiting from the monochromator. In practice we have found it convenient to define f'_x and f'_y by a pinhole about 0·45 mm in diameter.

Where possible, the crystal-to-monochromator distance s (or s') should be kept to a minimum, in order to maximize intensity. Only when required by the need to increase resolution (equation 2) should the camera be moved away from the monochromator exit pinhole.

4. Monochromatic radiation

The potential advantages of strictly monochromatic radiation for screenless X-ray photography are well known. The unwanted white-radiation background, as well as radiation streaks, are completely eliminated. Also, use of monochromatic radiation is expected to enhance useful crystal life, since the crystal is only exposed to radiation which potentially contributes to the measured diffraction pattern. Our experience with a number of protein crystals confirms this expectation. We have found that crystals can often be exposed ten times longer in a monochromatic beam than in a comparable nickel-filtered beam, before seeing equivalent radiation damage. [Also, for reasons not well understood, but reported informally by others, we find that radiation damage seems to be less for short, intense exposures than equivalent long, weak (or interrupted) exposures.]

The reputed disadvantages of monochromated radiation for oscillation photography are a reduction in intensity, relative to a nickel-filtered source, and limitations on resolution owing to 'fuzziness' of the diffracted spots (*e.g.* Arndt & Sweet, 1977). We have found that by use of an appropriate X-ray source, and by optimizing the collimation geometry, these disadvantages can be eliminated. In this section we discuss the use of the monochromator, *per se*, and how the need to collimate the monochromatic beam affects the choice of focal-spot size.

As a preliminary comparison, we recorded a series of oscillation photographs with a conventional rotating-anode generator (2·0 × 0·2 mm focal spot, 1·6 kW) with three different beam geometries: (1) nickel-filtered radiation with pinhole collimation; (2) a double mirror system (Harrison, 1968); (3) graphite-monochromatized radiation as described below. The resultant films were not measured, so that the following two conclusions are subjective. (1) There is no advantage in using a mirror–mirror system unless one is forced to do so by a cell dimension exceeding about 150 Å. This is in accord with the findings of Harrison, reported by Arndt & Sweet (1977). (2) A graphite monochromator with appropriate collimation produces by far the 'cleanest' pictures, but requires two to three times the exposure relative to the nickel-filtered beam. Resolution of cell edges up to 150 Å was not a problem. As discussed below, use of a larger focal-spot size can dramatically reduce the exposure time.

The reflection of X-rays from a vertical monochromator crystal is illustrated in Fig. 3(*a*). It is expected that a monochromator crystal will produce a pseudo-image of the X-ray source equidistant from the monochromator (*e.g.* see Fig. 5.13 of Arndt & Sweet, 1977) but, as Fig. 3(*a*) shows, such an image is not perfect. In addition, X-rays incident on the monochromator may penetrate 0·3 mm or so before being reflected, which will also blurr the focus. Photographs taken at increasing distances from the monochromator exit port do not reveal a sharp image of the focal spot. In addition, the reflected X-rays diverge continuously in the vertical plane as one moves away from the monochromator. This suggests that maximum intensity will be obtained by placing the monochromator crystal as close to the X-ray source as possible (as is common practice), and (other considerations aside) placing the camera as close as possible to the exit port of the monochromator housing.

When used in the manner described, the monochromator will produce an extended source of X-rays. If the monochromator crystal is mounted vertically, the width of this effective source will be about 0·6 mm or so, plus additional parasitic scattering, and the horizontal divergence of the reflected beam will originate from the monochromator rather than the focal spot (Fig. 3*a*).

In the vertical direction, the beam diverges from the focal spot (Fig. 1*b*). In addition, as pointed out to us by Dr H. Wyckoff, there is an additional divergence, α, owing to the mosaicity of the graphite crystal (Fig. 3*b*). Straightforward geometry shows that

$$\alpha = \frac{2\omega d_1 \sin\theta}{d_1 + d_2}, \qquad (5)$$

where d_1 is the focal-spot-to-monochromator distance, d_2 the monochromator-to-specimen-aperture distance, ω the mosaic spread and θ the Bragg angle for the graphite monochromator. In general, α will be about 0·06° or less.

Because the monochromator crystal provides such a broad source, it will give 'fuzzy' spots on the film unless either the distance from monochromator to protein crystal is increased, or additional collimation is introduced, or a combination of these is used, as discussed in the previous section. We now ask what can be done to maximize the reflected intensity from the monochromator itself. One obvious step, already mentioned, is to place the monochromator crystal as close as possible to the X-ray focal spot. The second important factor is focal-spot size. The objective is to have each point on the used area of the monochromator crystal reflect as many X-ray quanta as possible in directions which will reach the protein crystal. In the horizontal direction the two factors which need to be considered are the pseudo-focusing of the monochromatic beam (Fig. 3*a*), and the limitations imposed by the mosaic spread of the monochromator crystal. As shown in Fig. 1(*a*), the pseudo-focus lies between the monochromator aperture and the specimen aperture, and the size of the pseudo-focus can be usefully increased until it fills the limiting cone between the two apertures. Since the two apertures are usually of comparable size, the maximum useful width of the pseudo-focus, which in turn is approximately equal to the size of the focal spot itself, is equal to f'_x (or a'_x), *i.e.* about 0·45 mm in practice. The effect of the mosaic spread of the graphite monochromator is to limit the width of the focal spot which can be 'seen' by a given point on the monochromator. If a monochromator mosaic spread of 0·4° is assumed, the limiting focal-spot width for a rotating-anode generator with a typical focal-spot-to-monochromator distance of 80 mm and a vanishingly small monochromator aperture is 0·56 mm. As the monochromator aperture f'_x is increased in size, the focal spot could, in principle, be increased by the same amount, although there is clearly no gain in intensity when the pseudo-focus exceeds the limits described above (*i.e.* about 0·45 mm). In other words, it is usually the collimation of the X-ray beam rather than the mosaic spread of the monochromator which determines the maximum useful size of the focal spot. Where the X-ray generator design allows, it is clearly advantageous to increase the focal-spot size to equal this value, since a larger focal spot can provide a greater total flux than a small spot.

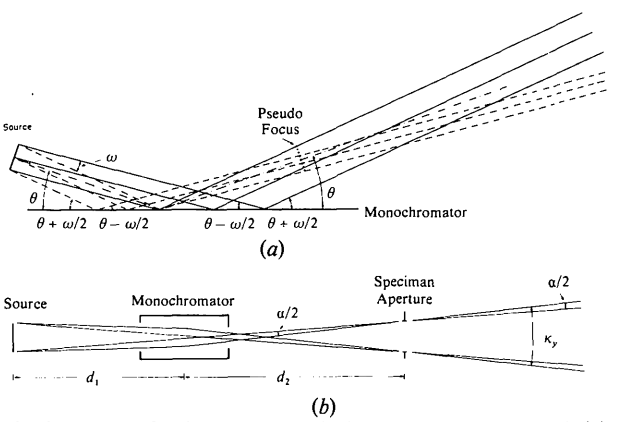

Fig. 3. X-ray reflection from a vertical monochromator crystal. (*a*) Plan. The angle ω is the mosaic spread of the monochromator. (*b*) Elevation. As explained in the text, α is the additional divergence caused by the mosaic spread of the monochromator. For simplicity, only the rays which define the maximum divergence are drawn.

In the vertical direction (Figs. 1*b*, 3*b*), the beam diverges primarily from the focal spot, and the monochromator can be effectively ignored. Here, useful intensity is proportional to the height f_y of the focal spot, and the upper limit on f_y is determined by the desired vertical crossfire (equation 3). As discussed previously, a focal spot of 0·5 mm will result in a vertical crossfire of about 0·29° or less, which is quite acceptable.

These arguments suggest that, with typical collimation geometry, the optimum focal-spot size for use with monochromatized radiation is about 0·5 × 0·5 mm, as seen from the X-ray port. This contrasts with normal pinhole collimation, where diffracted intensity, defined as maximum film darkening, is claimed to depend strictly on source brightness rather than total flux (Arndt & Sweet, 1977). In practice we have found that an Elliott GX-21 generator running at 6 kW on a 0·5 × 5 mm focal spot reduces exposure times by a factor of four relative to a generator running at 1·6 kW on a 0·2 × 2 mm focal spot. This factor of four more than offsets the factor of two to three increase in exposure which is normally considered to be necessary to obtain comparable intensities with monochromatized radiation relative to β-filtered radiation (Arndt & Sweet, 1977). The above argument suggests that a monochromatized beam from a high-brilliance

sealed X-ray tube run at 1·5 kW with a focal spot of 0·4 × 8 mm ought to have an intensity comparable with a rotating-anode source run at 1·6 kW, although the sealed tube will lose intensity because of its shallow take-off angle.

An oscillation photograph for thermolysin, showing the resolution of spots along a horizontal c axis of 131·4 Å and the rectangular spot shape produced by an adustable collimator, is shown in Fig. 4. The crystal used for this photograph was a hexagonal prism 1·4 mm in the horizontal direction, and 0·45 mm in diameter.

5. Intensity measurement

The system we have developed for intensity measurement is based on that of Rossmann (1979). One of the advantages of this approach is that the alignment of the crystal is determined automatically from the same film that is used for intensity measurement. The method was developed initially for virus photography, where only a single exposure could be taken of each crystal (Schutt & Winkler, 1977; Rossmann, 1979), and contrasts with the alternative approach in which additional still or other alignment photographs are used to determine the exact orientation of the crystal (Xuong & Freer, 1971; Arndt *et al.*, 1973; Nyborg & Wonacott, 1977; Wilson & Yeates, 1979). Clearly, the reliance on additional photographs for determination of crystal alignment has several disadvantages (Schwager, Bartels & Jones, 1975). One way of determining crystal alignment from an oscillation photograph is to identify manually a number of the partially recorded reflections and to base the alignment on these reflections (Schwager *et al.*, 1975; Jones, Bartels & Schwager, 1977). This method reduces the amount of computing, but requires manual intervention for each film. The Rossmann (1979) procedure is entirely automatic, although it does require additional computing. As described below, we have found it desirable to modify Rossmann's procedure somewhat for use with protein (as opposed to virus) crystals. In the following discussion we discuss only those aspects of our procedure which differ from that described by Rossmann.

The first step is to find the transformation between the scanner coordinate frame and the camera coordinate system, *i.e.* the Q matrix of Rossmann (1979). As described previously, this is greatly simplified by the use of alignment pins incorporated within the cassette. The accurate determination of the Q matrix uses whole reflections, and differs slightly from Rossmann in that the Q matrix is constrained to be orthogonal. In other words we preserve the 90° angle and the relative lengths of the vertical and horizontal axes of the scanner coordinate frame, rather than trying to use the Q matrix to allow for errors in the crystal-to-film distance and anisotropic shrinking of the film. We refine separately the crystal-to-film distance and a parameter correcting for any vertical misalignment

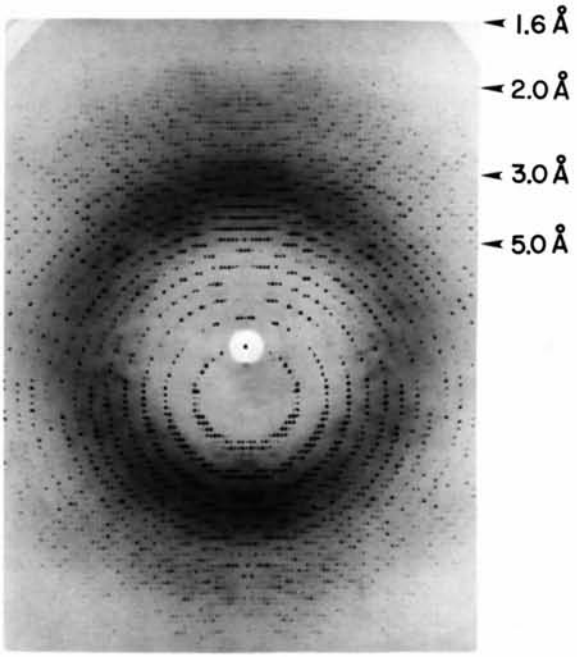

(*a*)

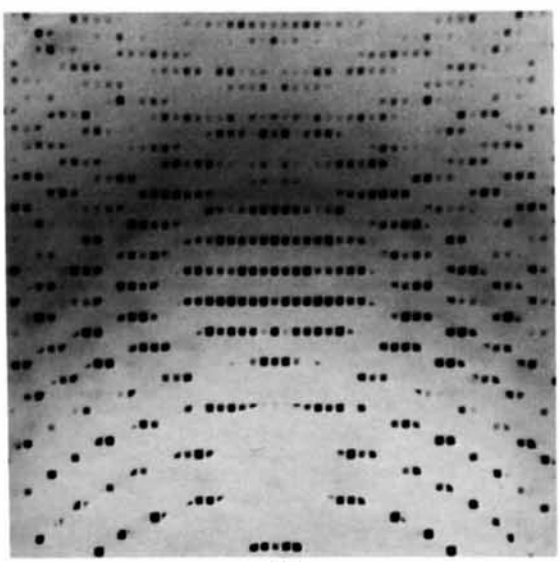

(*b*)

Fig. 4. (*a*) Oscillation photograph for thermolysin. The arrows indicate the resolution in ångströms in the central region of the film. Unit-cell dimensions $a = b = 94·2$, $c = 131·4$ Å. Crystal 0·45 × 0·45 × 1·4 mm. Collimator aperture 0·30 mm (horizontal), 0·40 mm (vertical). Crystal-to-film distance 80 mm. Focal spot approximately 0·5 × 5·0 mm; 39 kV, 140 mA, exposure time 6 h. Oscillation range 1·0°. Because of the cylindrical cassette, the reflections lie on parallel vertical lines (layer lines). (*b*) Enlargement showing the central region of the film from about 25 to 2·3 Å resolution.

between the cassette cylinder axis and the spindle axis (this being the most difficult alignment adjustment to make on the cassettes).

Our most significant difference from the procedure of Rossmann is in the refinement of the orientation matrix A relating the crystal alignment to the camera coordinate frame. The crystal orientation is defined by rotations about three axes, the vertical X axis, the horizontal Y (spindle) axis, and the horizontal Z (X-ray beam) axis. Rotations about the Z axis cause a bodily rotation of the X-ray pattern on the film, and are easily determined from the positions of the whole spots on the film. Rotations about Y, the spindle axis, cause additional reflections to appear at one end of the crystal oscillation range, and other reflections to be 'lost' at the other extreme of the oscillation range. This effect is most noticeable along the equator (vertical axis) of the film. Rotations about the vertical axis X cause some reflections, most noticeably near the meridian (horizontal axis), to begin to be lost, but others will begin to appear.

Rossmann's approach is to consider small rotational increments of the crystal about the X and Y axes, assuming that the correct oscillation range and mosaic spread of the crystal are known. For each increment, any new reflection which would come into the reflecting position is noted, and the measured intensity of all such reflections is summed. Similarly, any reflections 'lost' are also noted. If, for a given increment, more intensity is gained than lost, then one continues to increment in that direction until the optimum orientation is reached, at which point the intensity gained minus intensity lost is a maximum (*i.e.* any rotation causes no significant intensity gain, but does cause a loss of intensity). Rossmann describes the method as a 'convolution' technique, meaning that one fits an expected 'window' of reflections to the intensity distribution which is actually observed on the film. Rossmann's procedure depends on the change in the intensity distribution at the leading edge and the trailing edge of the window (*i.e.* at the beginning and the ending of each lune of reflections on the film). As described below, we have found it desirable to base the orientation refinement on, essentially, the center of gravity of the intensity distribution within each lune. Our approach involves the following steps (see also the caption to Fig. 5).:

1. All reflections which occur in 0·1° oscillation ranges about the spindle axis are computed. Since, for the purposes of this computation, we choose 0° mosaicity, a reflection will not appear in more than one range.

2. The reflections in each range are measured, and the average intensity for that range is computed (Fig. 5*a*).

3. The center of gravity of intensity for the overall intensity distribution is taken as the new spindle setting angle φ_Y, and $\delta\varphi_Y$ is defined as the difference between this value and the previously assumed value of φ_Y.

For the X-axis refinement, the orientation angle φ_X is incremented in steps of 0·1°, and, for each value of φ_X, φ_Y is swept through its oscillation range and all reflections occurring within this range are summed and averaged (Fig. 5*b*). We have found it desirable to exclude reflections in the 90° sectors at the top and

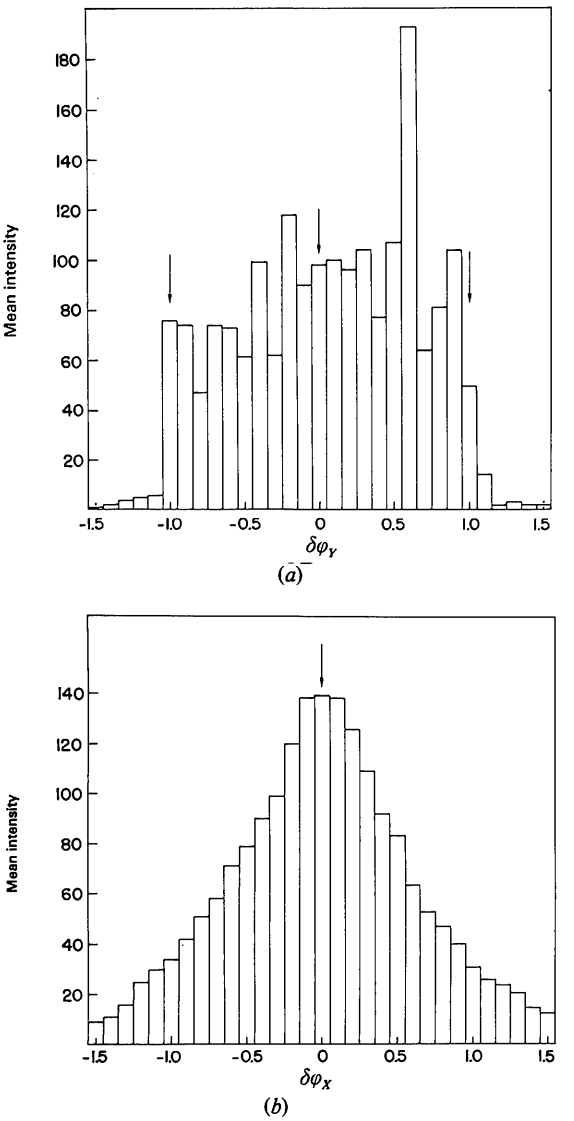

Fig. 5. Crystal orientation profiles for a typical T4 phage lysozyme oscillation film. Cell dimensions $a = b = 61{\cdot}2$, $c = 96{\cdot}8$ Å; oscillation range 2°; resolution for refinement 3·0 Å. (*a*) In the Y-axis refinement the crystal orientation is incremented in steps of 0·1° and the average reflection intensity for each increment is plotted. The theoretical limits of the oscillation range and the center of gravity of the intensity distribution are indicated. (*b*) For X-axis refinement, φ_X is incremented in steps of 0·1°, and, for each step, φ_Y is swept through the oscillation range of 2°. The plotted intensity is the average for all reflections within the 2° range, and the optimum value of φ_X is shown.

bottom of the film in order to eliminate reflections near the equator which would appear in several X-angle steps. (Conversely, in the Y-axis refinement we exclude reflections in the 90° sectors to the left and right of the film.) As with the Y-axis refinement, the optimum value of φ_X is taken to be the center of gravity of the intensity distribution (Fig. 5*b*). Cycles of refinement about X and Y are alternated, and refinement usually achieves a movement of less than 0·01° in $\delta\theta_X$ and $\delta\theta_Y$ per cycle (our criterion for completion) in less than five cycles.

There are several advantages to this method. Both Rossmann's procedure and our modification depend on all reflections having 'average' intensity. In practice, of course, this means a large enough sample of reflections must be used that the random variations in both the number of reflections and their intensities in different regions of reciprocal space are smoothed out. Our modification makes use of virtually all reflections (at least for Y refinement) in computing the weighted average of the intensity *vs* orientation, whereas Rossmann uses only those which are gained or lost on rotations as small as 0·01°. This may be satisfactory for a virus crystal, but, at least in our experience, gives less-consistent results for typical protein crystals, especially those with smaller unit cells.

Another major advantage is that the proposed method does not assume a knowledge of the mosaic spread in advance, whereas Rossmann's approach is rather sensitive to the choice of mosaicity. This can be seen from the representative profile shown in Fig. 5(*a*). If, for instance, too large a mosaicity is chosen, then the 'search window' will be wider than the actual profile, and all reflections gained or lost on rotation of the crystal will be outside the oscillation range and in the noise region. On the other hand, too small a mosaic spread will place the 'search window' completely inside the actual profile, so that again the optimum position will not be well determined.

A comparison of the refinement techniques for two different proteins is given in Table 1. The angles $\delta\theta_X$ and $\delta\theta_Y$ are the refined orientation angles relative to the approximate starting values. In the table, $\delta\theta_X$ and $\delta\theta_Y$ are calculated for a series of contiguous oscillations of the same crystal. If the crystal has not slipped during the series of exposures, the values of $\delta\theta_X$ and $\delta\theta_Y$ should be the same for each exposure, and the variations in $\delta\theta_X$ and $\delta\theta_Y$ give an estimate of the accuracy of the determination of the crystal orientation angles. For simplicity of comparison, the values of $\delta\theta_X$ and $\delta\theta_Y$ quoted in Table 1 are not the actual calculated values, but are the differences in $\delta\theta_X$ and $\delta\theta_Y$ from their mean value for the series of films. Two different situations are illustrated in Table 1. The first example is nine contiguous films of a platinum derivative of goose lysozyme (Grütter, Rine & Matthews, 1979), with space group $P2_1$ and cell dimensions $a = 38·3$, $b = 65·7$, $c = 45·2$ Å, $\beta = 116°$. The second example is four contiguous films of a bacteriochlorophyll protein (Matthews, Fenna, Bolognesi, Schmid & Olson, 1979), cell dimensions $a = b = 112·4$, $c = 98·4$ Å, space group $P6_3$. For the larger bacteriochlorophyll protein cell, the proposed refinement procedure gives results which are somewhat more consistent than Rossmann's procedure, although there is little to choose between the two techniques. However, in the case of the smaller goose lysozyme cell, which has far fewer reflections on each film pack, the proposed procedure is clearly superior. Here, the r.m.s. variation in both $\delta\theta_X$ and $\delta\theta_Y$ is 35% lower for the proposed method than for Rossmann's method. It appears that Rossmann's method works best when there is a large number of reflections on the film, and, therefore, a reasonable number of reflections close to the edge of each lune. It is these 'edge' reflections which are critically important in Rossmann's orientation procedure. In contrast, the proposed method uses all the reflections in each lune, and the accuracy does not seem to depend very much on the number of reflections on the film. In Table 2 we give the variation in the crystal orientation angles for several different proteins. The results suggest that the typical uncertainty in the calculated orientation angles φ_X and φ_Y is about 0·05°. As proposed by Schutt & Winkler (1977) and Rossmann (1979), it is also possible to obtain higher precision by 'post-refinement' techniques, although this is not so important when one can add together partial reflections recorded from the same crystal on successive film packs. Where a

Table 1. *Comparison of crystal orientation methods*

The values of $\delta\theta_X$ and $\delta\theta_Y$ give the refined values of the crystal orientation angles relative to assumed, approximate starting values of θ_X and θ_Y, determined from a series of contiguous oscillations of the same crystal. For ease of comparison, the quoted values of $\delta\theta_X$ and $\delta\theta_Y$ are the differences from the average, rather than the raw calculated values.

Crystal	Rossmann procedure		Proposed procedure	
Goose lysozyme	$\delta\theta_X$ (°)	$\delta\theta_Y$ (°)	$\delta\theta_X$ (°)	$\delta\theta_Y$ (°)
Film 1	−0·031	−0·171	0·033	0·008
2	0·054	0·186	0·022	0·027
3	−0·116	0·109	−0·072	0·069
4	−0·016	0·009	0·010	−0·091
5	0·014	0·069	0·037	0·095
6	−0·026	0·039	0·004	−0·024
7	0·049	0·049	0·021	0·097
8	0·024	−0·096	−0·026	−0·051
9	0·049	0·174	−0·024	−0·011
R.m.s. value	0·051	0·117	0·033	0·073
Bacterio-chlorophyll protein	$\delta\theta_X$ (°)	$\delta\theta_Y$ (°)	$\delta\theta_X$ (°)	$\delta\theta_Y$ (°)
Film 1	−0·008	0·037	−0·039	−0·041
2	0·042	0·051	0·021	0·041
3	−0·008	−0·109	−0·004	−0·061
4	−0·028	0·021	0·023	0·062
R.m.s. value	0·026	0·064	0·025	0·052

Table 2. *Accuracy of crystal orientation*

Crystal	Number of contiguous films	R.m.s. $\delta\theta_X$ (°)	R.m.s. $\delta\theta_Y$ (°)
Goose lysozyme	9	0·033	0·073
Bacteriochlorophyll protein: Run 1	4	0·025	0·052
Bacteriochlorophyll protein: Run 2	8	0·038	0·042
T4 phage lysozyme	5	0·023	0·032
Group-specific protease	20	0·054	0·082
Thermolysin: Run 1	7	0·094	0·036
Thermolysin: Run 2	9	0·022	0·023

contiguous set of films is available, as in Tables 1 and 2, it is possible, in principle, to increase the precision by using the average of the orientation angles determined for the set, rather than the individual values. We tested the potential advantage of such averaging by processing a contiguous set of phage lysozyme films in two ways. In one case the individually determined orientation parameters for each film were used, and in the second case a constant overall average orientation was used for all the films. When the respective data sets were merged together, the respective R values were essentially identical. In the latter case the merged data set contained about 1% more reflections because, with constant orientation parameters, each film exactly matches the adjacent films in the set, whereas, with individually determined orientation parameters, a few partially recorded reflections on adjacent films are 'lost'. On balance, there seems to be little to be gained by averaging the crystal orientation parameters and reprocessing all the films.

The proposed method for determining the crystal orientation will routinely converge to the correct solution if the assumed orientation of the crystal is correct within a degree or so. The range of convergence has not been tested fully, but we have, on occasion, seen correct convergence where the assumed orientation was in error by 3°. In cases where the alignment of the crystal is in doubt, it is desirable to carry out an initial refinement with the low-angle data, *e.g.* to 5 Å resolution, before including the high-resolution data.

As discussed by Rossmann (1979) and others (Diamond, 1969; Ford, 1974), it is desirable to use profile fitting to improve the accuracy of the weak reflections, to estimate standard deviations, and also to provide criteria for the rejection of doubtful measurements. Our procedure follows that described by Rossmann. Intensities of fully recorded reflections are estimated by comparison with a profile which varies across the film. Partially recorded reflections are measured by summing optical densities within designated peak and background areas. Partial reflections on adjacent films are summed, but are usually ignored if the reflection extends over more than two exposures. Variation in spot shape is taken into account by means of the profile shape, which can change smoothly across the film. Because of the cylindrical geometry, spot-shape variation is less than for a flat or V-shaped cassette. Also, the obliquity correction varies least for cylindrical geometry, in which case it depends only on the distance from the equator. The necessary obliquity corrections are given by Wonacott (1977), although two errors need to be corrected. In equation (7.32), $A(\beta)^2$ should be replaced by $A(\beta)$, and in equation (7.33), $A(\beta)^n$ should be replaced by $A(\beta)$.

Along with other investigators we have found that the measured intensities of partially recorded reflections tend to be systematically higher than the fully recorded reflections, especially for the weak data (Irwin, Nyborg, Reid & Blow, 1976; Wilson & Yeates, 1979). It is important, when measuring weak data, not to discard reflections for which the measured intensity is negative. Such negative values should be kept and averaged with measurements of the reflection from other films, otherwise the weak reflections will be systematically overestimated. Since partial reflections occur on more films than do whole ones, they will, on average, be overestimated by more than the whole ones. The inclusion of the 'negative' reflections reduces, but does not eliminate the systematic overestimation of the partial reflections. The overestimation is given by R_{bias} (*cf.* Irwin *et al.*, 1976), where

$$R_{\text{bias}} = 100\frac{\sum(\langle I_F\rangle - I_P)}{\sum\langle I_F\rangle}. \qquad (6)$$

$\langle I_F\rangle$ is the average intensity of the fully-recorded reflections and I_P the intensity determined by summing partially recorded reflections. In a test with the 1·8 Å resolution data set for T4 phage lysozyme, the value of R_{bias} when all negative intensity measurements were excluded was −7·6%. Including the negative measurements reduced the bias value to −3·3%.

Some representative data processing statistics are given in Table 3. The R values depend on several factors such as the resolution and the redundancy of the data, but they do give an indication of the overall quality of the data. In most cases the crystals used were about 0·4 to 0·5 mm in cross section, although the goose lysozyme crystals were thinner (0·4 × 0·4 × 0·15 mm). The lower R value for the goose lysozyme crystals may be due in part to the lower absorption in this case. In contrast, the phage lysozyme crystals were equilibrated with electron-dense phosphate solutions which increased the absorption. The relatively high R value for the bacteriochlorophyll protein is due in part to the large number of films and the high redundancy (approximately threefold) of the data. As an independent test of the quality of the oscillation data we compared the thermolysin data, measured to 1·6 Å,

Table 3. *Data processing statistics*

Protein	Resolution (Å)	Films	Crystals	Total reflections	Unique reflections	R^*_{sym}	R^*_{merge} (Including partials)	R^*_{merge} (Deleting partials)
Thermolysin	1·6	48	5	95 806	32 660	5·0	8·8	7·1
T4 phage lysozyme	1·9	28	4	32 410	13 466	6·7	11·6	10·2
Mutant T4 lysozyme, N14	2·1	19	2	19 126	10 502	–	9·5	7·9
Bacteriochlorophyll protein	1·9	76	9	126 269	46 764	4·6	11·6	10·0
Goose lysozyme	2·0	32	2	18 739	10 959	–	5·2	–
Cro repressor	2·4	15	2	18 940	11 987	–	7·6	6·8

* $R = 100 \sum |I - \bar{I}| / \sum I$. R_{sym} is the R value for symmetry-related intensities recorded on the same film, and the value quoted is the average over all films in the data set. R_{merge} gives the agreement between intensities measured on different films.

with a previous data set collected to 2·3 Å resolution by precession photography (Colman, Jasonius & Matthews, 1972). For the 11 824 reflections common to the two sets of data the R value on intensities was 6·6%. Similarly, the R value for 6500 reflections common to a 2·4 Å resolution precession data set and a 1·8 Å resolution oscillation data set for T4 phage lysozyme was 10·8%. For the bacteriochlorophyll protein, 15 000 common reflections to 2·8 Å resolution had an R value of 9·8%. Recently, the oscillation data collection system has been used to determine the structure of the cro repressor protein from bacteriophage λ to 2·8 Å resolution (Anderson, Ohlendorf, Takeda & Matthews, 1981).

We are particularly grateful to Dr Robert Huber for copies of his modifications to the Enraf–Nonius precession camera and cylindrical cassette, on which the system described here is based. Also, we are very grateful to Dr Michael Rossmann for his film measurement program, and numerous discussions on its use. We also thank Dr Philip Evans for his film-merging program, Dr Harold Wyckoff for a discussion on monochromatization and collimation, and the Machine and Electronics Shops at the University of Oregon for designing and constructing the oscillation system.

This work was supported in part by grants from the National Science Foundation (PCM-8014311) and the National Institutes of Health (GM 20066; GM 21967); by a PHS Postdoctoral Fellowship (GM 07221) to MFS and a Damon Runyon–Walter Winchell Cancer Fund Postdoctoral Fellowship (DRG-303-F) to DHO; and by a grant from the M.J. Murdock Charitable Trust.

References

ANDERSON, W. F., OHLENDORF, D. H., TAKEDA, Y. & MATTHEWS, B. W. (1981). *Nature (London)*, **290**, 754–758.

ARNDT, U. W., CHAMPNESS, J. N., PHIZACKERLEY, R. P. & WONACOTT, A. J. (1973). *J. Appl. Cryst.* **6**, 457–463.

ARNDT, U. W. & SWEET, R. M. (1977). In *The Rotation Method in Crystallography*, edited by U. W. ARNDT & A. J. WONACOTT, pp. 43–62. Amsterdam: North-Holland.

ARNDT, W. & WONACOTT, A. J. (1977). *The Rotation Method in Crystallography*. Amsterdam: North Holland.

COLMAN, P. M., JANSONIUS, J. N. & MATTHEWS, B. W. (1972). *J. Mol. Biol.* **70**, 701–724.

DIAMOND, R. (1969). *Acta Cryst.* A**25**, 43–55.

FORD, G. C. (1974). *J. Appl. Cryst.* **7**, 555–564.

GRÜTTER, M. G., RINE, K. L. & MATTHEWS, B. W. (1979). *J. Mol. Biol.* **135**, 1029–1032.

HARRISON, S. C. (1968). *J. Appl. Cryst.* **1**, 84–90.

HUXLEY, H. E. (1953). *Acta Cryst.* **6**, 457–465.

IRWIN, M. J., NYBORG, J., REID, B. R. & BLOW, D. M. (1976). *J. Mol. Biol.* **105**, 577–586.

JONES, A., BARTELS, K. & SCHWAGER, P. (1977). In *The Rotation Method in Crystallography*, edited by U. W. ARNDT & A. J. WONACOTT, pp. 105–118. Amsterdam: North-Holland.

LOVE, W. E., HENDRICKSON, W. A., HERRIOTT, J. R., LATTMAN, E. E. & MCCORKLE, G. L. (1965). *Rev. Sci. Instrum.* **36**, 1655–1656.

MATTHEWS, B. W., FENNA, R. E., BOLOGNESI, M. C., SCHMID, M. F. & OLSON, J. M. (1979). *J. Mol. Biol.* **131**, 259–285.

NYBORG, J. & WONACOTT, A. J. (1977). In *The Rotation Method in Crystallography*, edited by U. W. ARNDT & A. J. WONACOTT, pp. 139–152. Amsterdam: North-Holland.

REEKE, G. N. JR (1977). In *The Rotation Method in Crystallography*, edited by U. W. ARNDT & A. J. WONACOTT, pp. 33–42. Amsterdam: North-Holland.

ROSSMANN, M. G. (1979). *J. Appl. Cryst.* **12**, 225–238.

SCHUTT, C. & WINKLER, F. K. (1977). In *The Rotation Method in Crystallography*, edited by U. W. ARNDT & A. J. WONACOTT, pp. 173–186. Amsterdam: North-Holland.

SCHWAGER, P., BARTELS, K. & JONES, A. (1975). *J. Appl. Cryst.* **8**, 275–280.

WILSON, K. & YEATES, D. (1979). *Acta Cryst.* A**35**, 146–157.

WONACOTT, A. J. (1977). In *The Rotation Method in Crystallography*, edited by U. W. ARNDT & A. J. WONACOTT, pp. 75–103. Amsterdam: North-Holland.

XUONG, N. H. & FREER, S. T. (1971). *Acta Cryst.* B**27**, 2380–2387.